Spectroscopy 22 (2008) 223–234
DOI 10.3233/SPE-2008-0351
IOS Press

FTIR-ATR biosensor based on self-assembled phospholipids surface: Haemophilia factor VIII diagnosis

Ahmed Aamouche * and Erik Goormaghtigh
Laboratory for the Structure and Function of Biological Membranes, Center for Structural Biology and Bioinformatics, Free University of Brussels, Campus Plaine CP206/2, 1050 Brussels, Belgium

Abstract. We report a new generic device suitable for the investigation of biological interactions by means of Fourier Transform Infrared (FTIR) spectroscopy. The research is focused on multi reflected evanescent optical radiation through a chemically modified surface of the attenuated total reflection (ATR) element (silicon or germanium). Using a wet chemistry approach, the original method is based on grafting of a bifunctional binding molecule (N-hydroxysuccinimidyl ester forms) at the surface of the Si or the Ge crystals. The functionalized surface permits then the foundation of different types of self-assembled phospholipid membranes. The obtained sensors allow the detection, in infrared spectral domain, of any perceptible molecular interaction or structural changes. The key experimental result concerns the coagulation factor VIII (F_{VIII}). The principle of the diagnostic is related to the ability of F_{VIII} molecules to bind specifically to phosphatidylserine (PS) membrane.

Keywords: Biosensors, self-assembled lipid membranes, FTIR-ATR spectroscopy, ligand–receptor binding, protein–lipid interactions, factor VIII, haemophilia

1. Introduction

FTIR (Fourier transform infrared) spectroscopy is one of the most powerful techniques for structural and spectral direct recognition of biological materials and their interactions [1]. The biological molecules are primarily studied in aqueous solutions. In order to analyse the FTIR spectra, the main problem one should overcome is the strong water absorption. In combination with the attenuated total reflection (ATR) method, FTIR spectroscopy eases this effect and strengthens the signal to noise ratio [2]. The Internal Reflection Element (IRE) plays a major function in the ATR system. On the one hand, the IRE allows the multiplication of the number of reflections, and on the other, a portion of the IR light penetrates the IRE surface and probes the response of the highly concentrated molecules lying close to the interface.

Optical sensors have concentrated significant attention during the last decades [3]. These systems are based on several principles as reflectance, transmittance, absorption, ellipsometry or fluorescence. They permit a quantitative determination of one or more fundamental characteristics of the optical radiation like amplitude, photon energy, phase or polarization. Currently, there is a pressing need for new sensors that can detect a variety of compounds, ranging from simple ions to complex molecules and even microorganisms. The devices should then offer superior criteria concerning sensitivity, speed, reversibility and selectivity.

*Corresponding author (current address): Département des sciences de la matière, Faculté Polydisciplinaire, Université Cadi Ayyad, BP-4162, 46000, Safi, Morocco. Tel.: +212 64310123; Fax: +212 24669516; E-mail: a.aamouche@gmail.com.

One of the most significant biotechnological subjects is to investigate the protein–lipid interactions and their structural changes. As a model system of cell membranes, phospholipid bilayers were built on solid supports. The main method used so far for bilayer construction has been the famous Langmuir–Blodgett deposition on the IRE surface [4]. Due to the delicateness of the lipid film transfer; we tried a new biomembrane preparation procedure. This self-assembled bilayer technique utilizes, in permanent contact with IRE surface, the phospholipids liposome solution, and a number of heating–freezing cycles [5].

The first objective of this study is to ensure a perfect formation of the biomembrane, prior to any extra investigation. The article will reveal the utility and the stability of this construction. Our ultimate aim is to mimic the biological membrane allowing on the one hand to elucidate any structural change occurring in a protein, and on the other hand to create the foundation of a biosensor surface able to identify any peculiar molecular interaction. The example illustrating the efficiency of the new device will be the monitoring of the haemophilia factor VIII-phospholipids binding [6].

Factor VIII (F_{VIII}) is a large heterodimeric, multidomain plasma glycoprotein (m.w. $\approx$ 260 kDa), essential in the intrinsic pathway of blood coagulation [7]. The functional absence of F_{VIII} results in a severe X-linked bleeding disorder: haemophilia A. F_{VIII} acts as a cofactor in the Ca^{2+}- and phospholipids-dependent conversion of factor Xa by activated factor IX [8,9]. It consists of a light chain (m.w.: 80 kDa) and of a heavy chain (m.w.: 180 kDa), linked by a metal bridge involving a single copper ion. Proteolysis starting from the C-terminus leads to size heterogeneity of the heavy chain. In plasma, F_{VIII} is protected from proteolytic inactivation by its non-covalent binding to von Willebrand factor (vWF). Two binding sites have been identified: one at the N-terminus and the other in the C-terminal C2 domain of the F_{VIII} light chain. This domain is also implied in binding to phospholipids [10]. This point is of course crucial in the binding of the F_{VIII} to the membrane of platelets activated by thrombin or other antagonists [11]. The activation induces a reorientation of the phosphatidylserine (PS) and phosphatidylethanolamine (PE) from the inner to the outer layer of the membrane and leads to the formation of high affinity binding sites of F_{VIII} [12]. Based on recent studies, the molecular interaction between F_{VIII} and PS may provide a basis for the design of novel F_{VIII} lipidic structures for delivery applications [13]. Convincingly, circular dichroism and fluorescence studies indicate no significant changes in the secondary and tertiary structure of F_{VIII} associated with the membranes [14]. This means that any spectral changes in interacting F_{VIII} with membranes will only be linked to binding affinity. A short article reviews all the recent investigations on the structure, activity, and more importantly, stability of F_{VIII} [15].

Besides the classical detection methods based on immuno-affinity (Western blot, ELISA) [16], several biosensors have been developed to monitor the binding of F_{VIII} to phospholipid membranes or to provide a quantitative detection of the hemocompatibility factor. In particular, surface plasmon resonance (SPR) has been used to monitor the real-time protein interaction [10,17]. This technique makes use of changes in the refractive index of medium near a thin gold film evaporated on a glass substrate. The target or biological receptors are immobilized via the interaction with an amorphous Dextran matrix or via the interaction with an alkanethiol-based self-assembled monolayer. In SPR, the binding of the ligand to the receptor induces modifications of the refractive index in the immediate vicinity of the glass substrate. This yields a modification of the angle at which the minimum intensity of the reflected light is detected, i.e. of the resonance angle. The resulting detection measures the mass loading on the surface but does not provide a direct physico-chemical information about the ligand–receptor interaction. Pflegerl and coworkers [18] described a method using SPR and exploiting the covalent coupling of monoclonal antibodies against F_{VIII} throughout the primary amine groups to the carboxymethyl dextran surface (CM5 sensor, Biacore).

Recently [19], we have described the design of a new type of biodetection devices. These biosensors consisted in adequately functionalized IRE crystals and the detection of the ligand/receptors interactions was achieved using FTIR spectroscopy. The modification of the surface properties of the ATR elements by wet chemistry directly on the Germanium or Silicon surface avoided the evaporation or the sputtering of a thin metal layer and therefore considerably reduced the absorption of the incoming signal in the mid-infrared spectral range. The crucial steps in the surface functionalization were the activation of the semiconductor surface and the anchoring of small spacer molecules. Two approaches gave us satisfactory results: the first one consists of an oxidation of the Si or Ge surface and in the binding of alkylsilane molecules via hydrosilylation or hydrogermilation reactions [19]. The second one consists of the reduction of the IRE surface as Ge-H and the subsequent binding of alkene molecules to the activated surface. Another advantage of the method is that it allows not only a mass response of the ligand/receptor system but also identification of the ligand and the potential conformational transitions of the receptor, due to the use of the FTIR detection.

In the present work, we use this FTIR-ATR approach with chemically-modified Ge or Si crystals to detect the binding of F_{VIII} molecules, initially in solution, to phospholipid membranes in a complex media.

2. Experimental method

2.1. Materials

All chemicals were purchased from Sigma-Aldrich unless specified otherwise and used as received, without any further purification. Dipalmitoyl Phosphatidyl Choline (DPPC), 1,2-dioleoly-sn-glycero-3-phosphatidylserine (PS) and 1,2-dioleoly-sn-glycero-3-phosphatidylcholine (PC) were purchased from Avanti Polar Lipids. Recombinant F_{VIII} lyophilisates *Recombinate 250* was purchased from Baxter (Belgium). It was stabilized by human serum albumin (HSA). *Octanate 500* was purchased from Octapharma (Switzerland). Octanate is F_{VIII} concentrate from human plasma source and contains von Willebrand factor molecules to avoid coagulation factor proteolysis.

2.2. IRE surface functionalization

ATR crystal is of a trapezoidal shape ($50 \times 20 \times 2$ mm^3) with an internal angle of 45°. It was coated with a self-assembled monolayer of octadecyltrichlorosilane (OTS) as follows. The chemical bonding of molecules on Si substrates via the activation of the native SiO_2 layer was performed either by using an oxidation process to increase the density of SiOH groups at the surface or by using a reduction process to passivate the interface with a SiH layer. The Ge surface, with its native oxide layer, is more sensitive than the Si one to the oxidizing processes currently used to clean and activate them. Typically, the so-called Piranha solution (i.e. a H_2SO_4/H_2O_2 mixture in ratio 7:3 v:v at 150°C) strongly modifies the reflectance properties of the crystal surfaces. The oxidized surface blackens and turns out to be rapidly unusable for grafting. To avoid these drawbacks, an alternative grafting procedure has been proposed to clean the Ge surface and build a stable GeO_2 interface [19]. The IRE was immersed in HNO_3 (38%) during 1 min and rinsed in MilliQ water. Afterwards, the surface was activated in a mixture of H_2O_2 and ethanedioic acid (10%) during 5 min. Finally, the surface was abundantly rinsed under a MilliQ water flow. The procedure used to hydrophobize the ATR elements by OTS are derived from the work of Semal and coworkers [20]. The activated IRE were immersed in a solution of OTS (0.08% v:v) in a mixture of hexadecane and CCl_4 (ratio 7:3) during 16 h at 12°C.

2.3. Phospholipid membrane adsorption

The phospholipid membrane fragments were prepared from unilamellar vesicle solutions (SUV) as follows: DPPC, PS and PC liposomes were used at a concentration of 0.5 mg/l. They are dissolved in 200 µl of $CHCl_3$. The solvent was then evaporated under a nitrogen flux and the dry extract kept under vacuum during 10 h. A 1 ml amount of a 2 mM HEPES buffer solution (pH 7.3) was added. Small Unilamellar vesicles (SUVs) were prepared by sonicating the suspension. The functionalized IRE crystals were incubated with 200 µl of SUVs solution in the infrared cell during 6–10 h at 4°C. A FTIR spectrum was recorded just after the injection of the SUVs in the infrared cell and kept as a reference spectrum to monitor the formation of the lipid film. The procedure allows the lipid membrane to slowly and uniformly adsorb on the OTS-grafted IRE. At the end of the incubation, the excess of lipids was rinsed using 30 ml of buffer solution.

2.4. F_{VIII} molecules binding

A gradient solution of F_{VIII} (*Recombinate* or *Octanate*) in 2 mM HEPES was injected in the infrared cell. Typically, the concentration ranged from 0 to 0.25 mg/ml over 120 min. The experiments were run at room temperature (between 22 and 25°C).

2.5. FTIR experiments

FTIR-ATR spectra were obtained on a Bruker IFS55 spectrophotometer (Ettlingen, Germany) equipped with a MCT detector (broad band 12,000–420 cm^{-1}, liquid N_2 cooled, 24 h hold time) at a resolution of 2 cm^{-1} with an aperture of 3.5 mm and acquired in the double-sided, forward–backward mode. The spectrometer was placed on vibration-absorbing sorbothane mounts (Edmund Industrial Optics, Barrington, NJ). Two levels of zero filling of the interferogram prior to Fourier transform allowed the encoding of the data every 1 cm^{-1}. The spectrometer was continuously purged with dry air (Whatman 75-62, Haverhill, MA). For a better stability, the purging of the spectrometer optic compartment (5 l/min) and of the sample compartment (10–20 l/min) were dissociated and controlled independently by flow meters (Fisher Bioblock Scientific, Illkirch, France). The IRE trapezoidal Ge or Si plate (ACM, Villiers St. Frédéric, France) with an aperture angle of 45° yielded 25 internal reflections. The crystals were placed in an ATR holder for liquid sample with an in- and outlet (Specac, Orpington, UK). The liquid cell was placed at 45° incidence on a Specac vertical ATR setup. Furthermore, an elevator (WOW Company SA, Naninne, Belgium) under computer control made it possible to move the whole setup along a vertical axis. This allows the crystal to be separated in different lanes. A Masterftex tubing pump (Cole Palmer Instruments Company, Berchem, Belgium) was used for recirculating the desired solution into the liquid flow cell in a flow-through closed-loop mode. Typical flow speed was 4 ml/min. The software used for data processing was written in Matlab 7.1 program (Mathworks Inc., Natick, MA).

3. Results and discussion

3.1. OTS layer quantification

Well-ordered assemblies of phospholipid films are important for the success of our binding studies of F_{VIII}. For that reason, coated OTS thickness requests a quantitative evaluation procedure. To have an

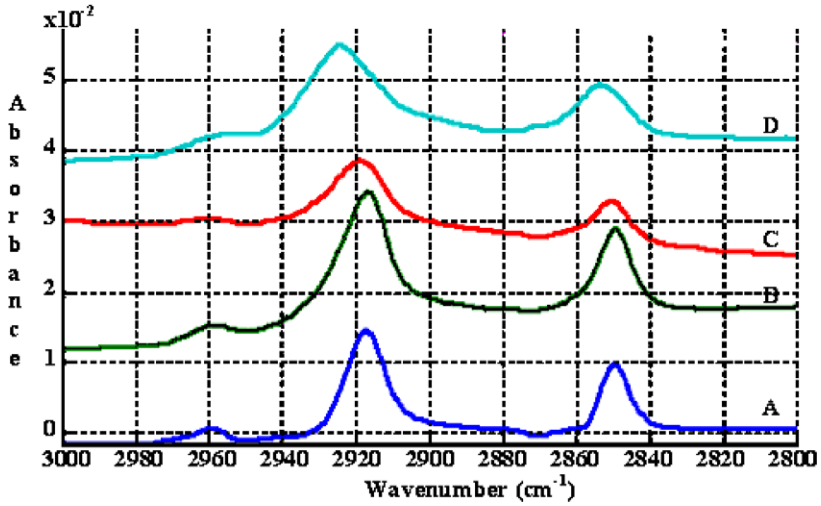

Fig. 1. FTIR spectra in CH_2 stretching range (2800–3000 cm^{-1}) obtained by LB method from a DPPC (A) and OTS (B) films on Ge ATR crystal. They are compared to spectra measured for Ge (C) and Si (D) crystals grafted with OTS.

idea about the order of magnitude of the amount of OTS grafted on Si or Ge crystals we adsorb two sort of films. Using Langmuir–Blodgett (LB) adsorption method we prepared DPPC and OTS monolayers. In both cases a single monolayer was transferred at constant surface pressure (30 mN/m) by vertically pulling the Ge crystal placed in a LB Lauda tank. The recorded FTIR absorbance spectra are shown in Fig. 1 in comparison with those obtained using OTS grafted crystals. First of all, the absorbance of the peaks assigned to the asymmetric CH_3 (2980–2950 cm^{-1}), asymmetric CH_2 (2950–2873 cm^{-1}), and symmetric CH_2 (2872–2812 cm^{-1}) stretching bands are slightly larger for the Si grafted with OTS film (curve D) than for the Ge one (curve C). This is obviously due to the efficiency of the oxidation reaction on Si. On the other hand the same bands are also larger for the OTS LB film (curve B) than for the DPPC LB monolayer (curve A). As OTS molecules are 18 carbons long (longer than DPPC chain), Fig. 1 strongly suggests that a compact OTS grafted monolayer was formed on the IRE surface.

3.2. Membrane adsorption control

In order to assure an excellent adsorption of phospholipids membrane over the OTS-grafted crystals, we fellow the incubation of a SUV solution prepared from DPPC. The IRE crystals were covered with 200 μl of SUVs solution in the infrared cell. A set of FTIR spectra (Fig. 2) was recorded just after the injection of the SUVs (as a reference; A spectrum) then after a process of freezing, rinsing and heating. The bands at 2917 cm^{-1} is assigned to $\nu_{as}(CH_2)$ and at 2849 cm^{-1} is assigned to $\nu_s(CH_2)$. Notice a shift of 5–8 cm^{-1} between the freezing–heating spectra related to the two different fluidity states of the bilayer. As shown in Fig. 3, the drawing of the integrated absorbance of the symmetric and anti-symmetric CH_2 stretching bands implies a well-organized film after the incubation procedure. The freezing step (B) increases the amount of the adsorbed SUVs while the rinsing step (C) indicates the stability of the constructed film. The heating process (D) decease the bands intensities which signify the expansion of the DPPC chains. At the end of the incubation, the excess of lipids can be rinsed (E) using the buffer solution. All these steps allow the lipid membrane to slowly and uniformly adsorb on the OTS-grafted IRE. We can then conclude that any membrane prepared at least after 6 or 10 hours of incubation will generate a good sensor surface.

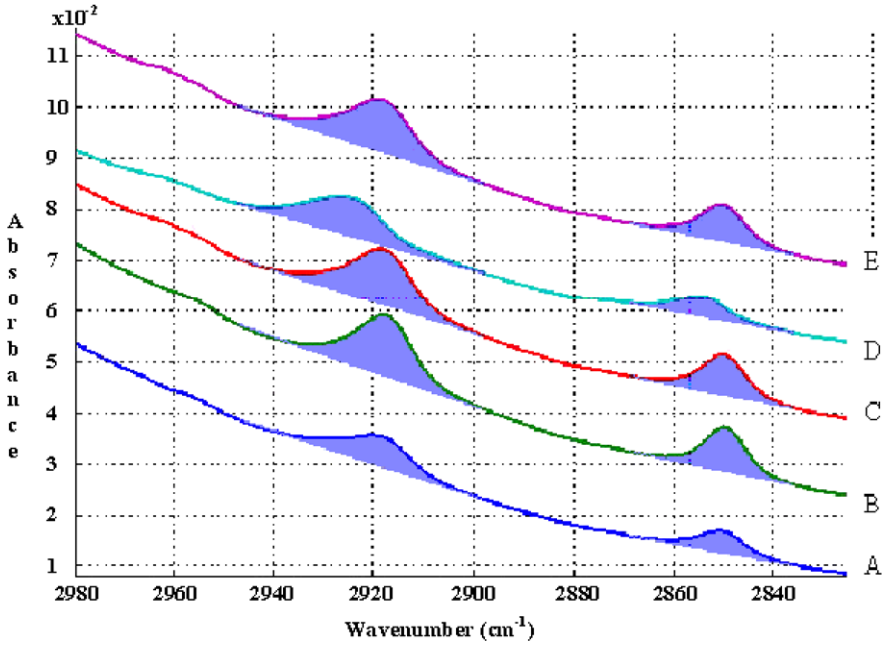

Fig. 2. FTIR spectra recorded during an incubation cycle of a DPPC membrane on a Ge surface. From the bottom to the top: (A) spectrum of injected DPPC SUVs; (B) after 10 h freezing at 5°C; (C) after 1 h buffer rinsing; (D) after 1 h heating at 50°C; (E) after 1 h buffer rinsing.

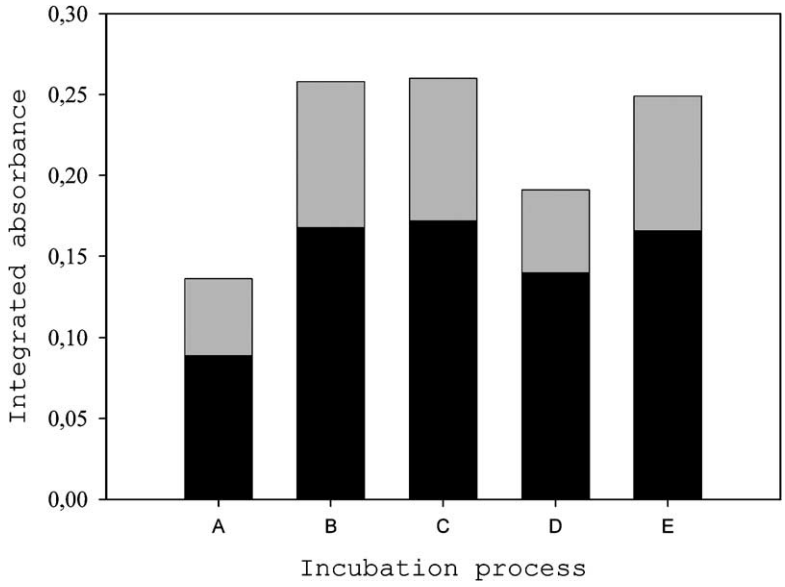

Fig. 3. Integrated intensities of symmetric (black) and asymmetric (grey) CH_2 stretching bands during the incubation processes (labelled A, B, C, D and E, see legend of Fig. 2).

In a second phase, to compare the amount of DPPC film adsorbed on Ge crystal, we recorded FTIR spectra for three preparation manners (Fig. 4). First we apply a simply immobilized and dried

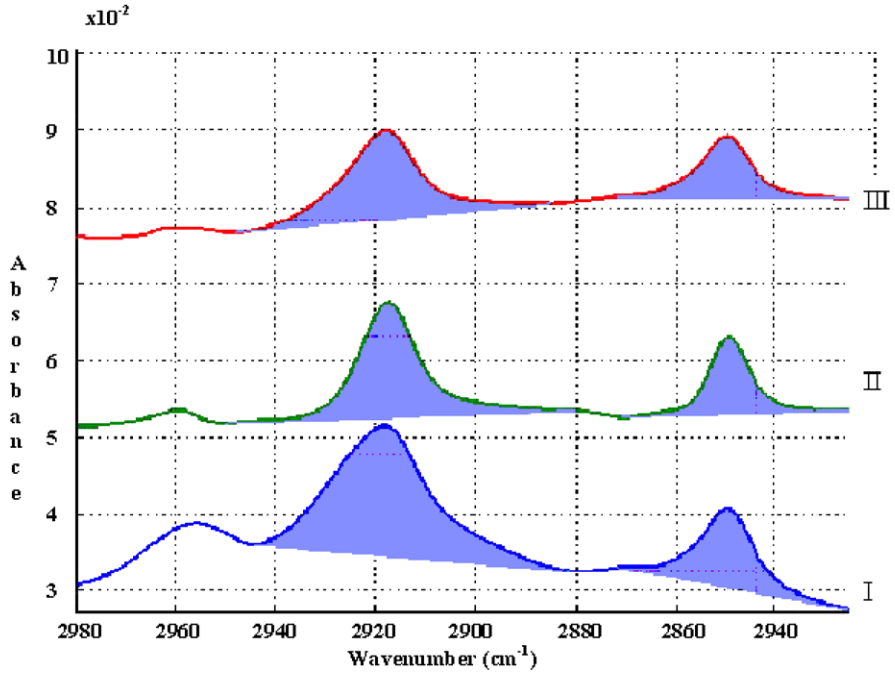

Fig. 4. Comparison of the CH_2 stretching bands intensities in cases of three different DPPC membranes: immobilized "dry" membrane (I), the LB deposed membrane (II) and the incubated "wet" membrane (III).

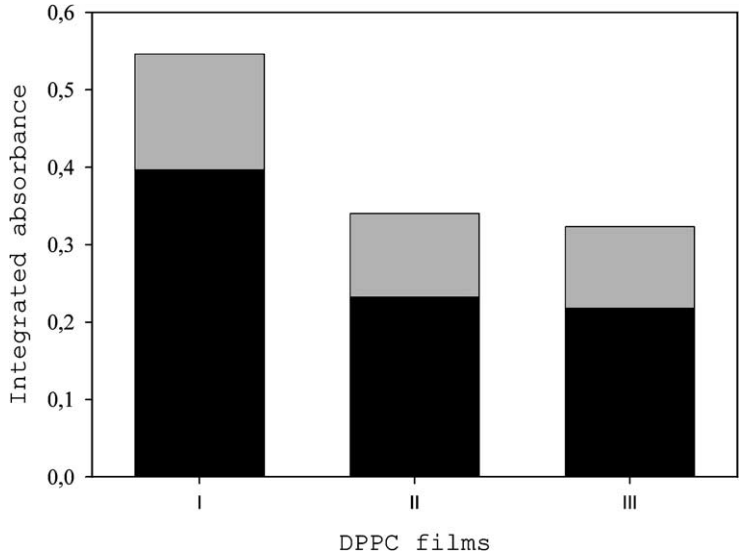

Fig. 5. Integrated intensities of CH_2 stretching bands (grey for $\nu_{as}(CH_2)$, black for $\nu_s(CH_2)$) of the three different DPPC membrane constructions (labelled I, II and III; see Fig. 4 legend).

film (I). The second approach uses a deposed LB film (II). The third protocol follow the incubation process (III) described above. The integrated absorbance for $\nu_{as}(CH_2)$ and $\nu_s(CH_2)$ are represented on Fig. 5. This chart shows that the incubated DPPC film has a quality close to that of an

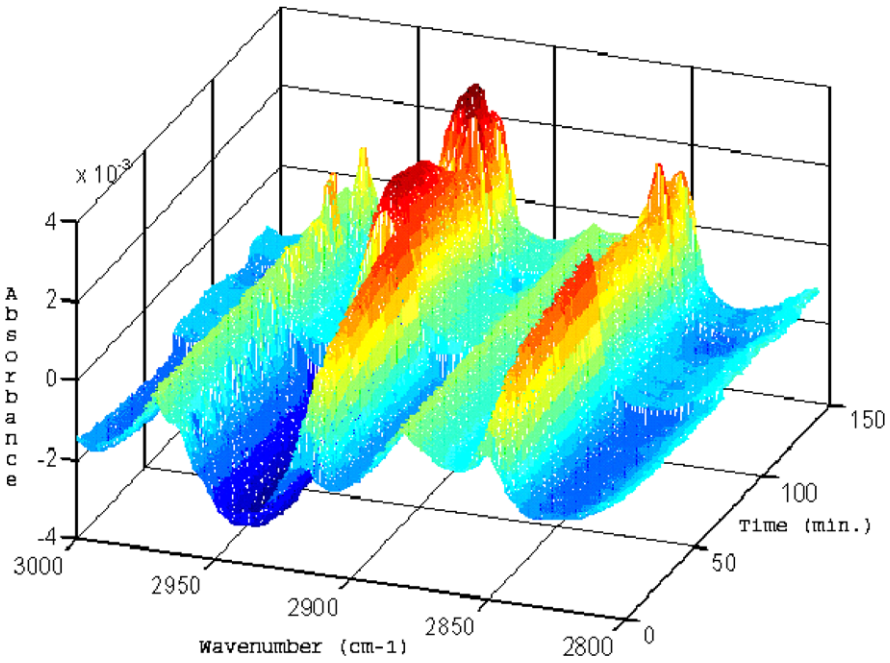

Fig. 6. 3-D representation of DPPC incubation FTIR spectra in CH_2 stretching region. After the SUVs injection, the incubation cycle applied here combines two freezing–heating steps and a buffer rinsing step of the membrane.

LB film. The immobilized film has a larger intensity but is inconvenient due to the lack of organization.

In order to optimize the incubation cycle exposed above we have multiplied the number of freezing–heating steps in smaller period of time before the rinsing stage. Figure 6 shows, in the spectral range of the CH_2 stretching bands, the 3-D representation of a set of 140 FTIR spectra recorded each minute during the steps of the incubation process. The time evolution of the integrated intensities of CH_2 stretching bands is illustrated on the Fig. 7. This experiment proved clearly that the multiplication of the freezing–heating steps did not improve considerably the amount of the lipids adsorbed. Also after just one hour of the first freezing step we might achieve the limit of the adsorption.

3.3. F_{VIII} binding experiment

In preliminary experiments, F_{VIII} solution in HEPES buffer was prepared from Recombinate 250. The samples were not a pure F_{VIII} solution. In particular, the solution contains recombinant F_{VIII} stabilized by human serum albumin (HSA). A series of experiments was therefore designed to control the non-specific interactions of HSA on the PS membranes. Solutions of Recombinate 250 and of a bovine serum albumin (BSA) were flown on an OTS-grafted ATR crystal incubated with PS or PC membranes. FTIR spectra were recorded every minute. In the 1400–1800 cm^{-1} spectral region, the raw data show that the intensity of the amide I (1680 cm^{-1}) and amide II (1550 cm^{-1}) absorption bands monitor the protein/membrane interaction. Figure 8 shows the time evolution of the amide I band intensity. The behaviours of the F_{VIII} and BSA solutions are obviously different. So, the PS membrane is selective with respect to the molecules in solution. As BSA molecules do not adsorb on the PS membrane fragments, it is possible to conclude that the data represented by the plain line in Fig. 8 correspond to the binding

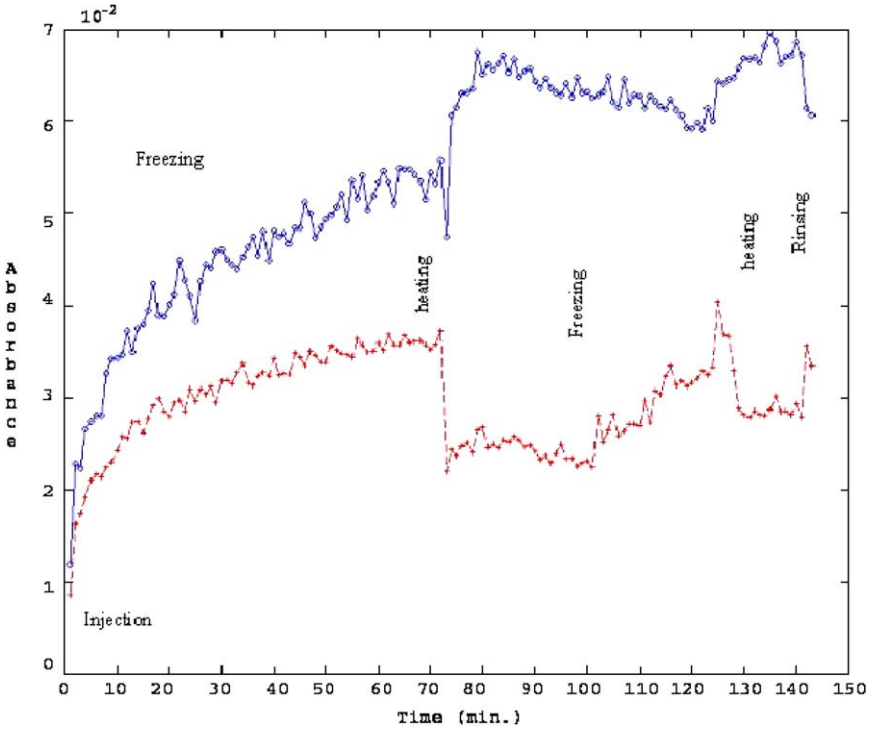

Fig. 7. The time evolution of the CH_2 stretching bands integrated intensities for the incubated DPPC membrane ($\nu_{as}(CH_2)$ for the upper curve, $\nu_s(CH_2)$ for the lower curve, see Fig. 6).

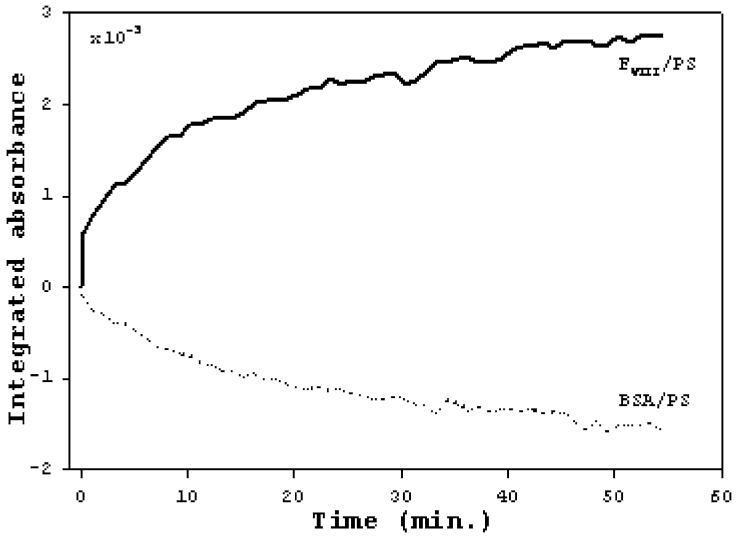

Fig. 8. The time evolution of the amide I band integrated intensities for separate solutions of F_{VIII} (*Recombinate 250*) and BSA flowed on a PS membrane surface.

of the F_{VIII} to the PS membrane fragments. This excludes the possibility of non-specific adsorption on the sensor.

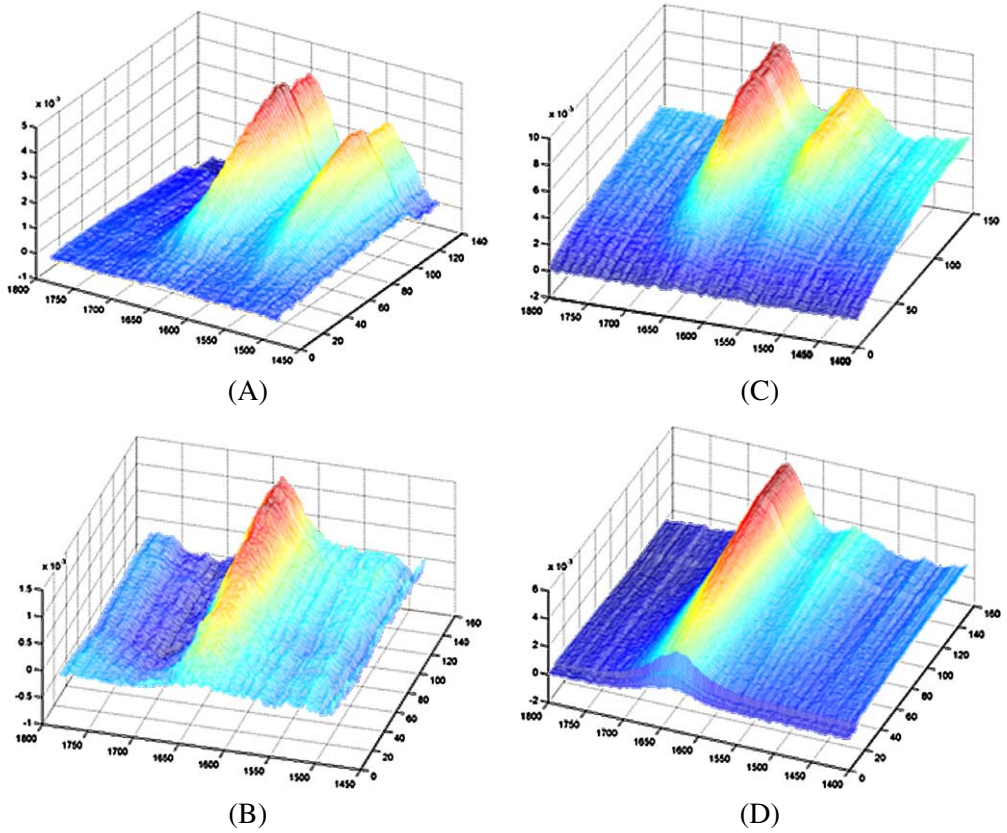

Fig. 9. Four series of 80 spectra recorded, at each 2 minutes, for F_{VIII} (*Octanate 500*) interacting with different lipid membranes in the amide I and amide II spectral range. The top series are for PS membranes on OTS-grafted Si (A) and OTS-grafted Ge (C) crystals respectively. The bottom series are for PC membranes on OTS-grafted Si (B) and OTS-grafted Ge (D) crystals respectively. For each set the last 20 spectra are recorded during the buffer rinsing phase.

Let us now consider the experiments monitoring the protein/membrane interactions resulting from the binding of the F_{VIII} to different types of membrane fragments. Two types of crystals (Ge and Si) were grafted with OTS and used as optical basis for the membrane adsorption. For each of them, two types of liposomes were considered: one with PS and the other with PC lipids. The F_{VIII} solution, prepared from Octanate 500 in 2 mM HEPES buffer, was progressively injected in the ATR cell, as a solution gradient ranging from 0 to 0.25 mg/ml during 120 min. A FTIR spectrum was then recorded every 2 min. Figure 9 represents all the spectra, in the amide I and amide II absorption range, for the Si (curves A and B) and the Ge (curves C and D) crystals. The time evolution of the amide II absorption bands is represented in Fig. 10(A) for the Si case and in Fig. 10(B) for the Ge one. For the sensors based on the Si, the binding of the F_{VIII} occurs only on the PS membranes. The control experiment with PC membranes shows that the protein does not bind to the phospholipids, as evidenced by the lack of growth of the amide II band. Concerning the sensors using Ge, our results show a preferential binding of the F_{VIII} molecules on the PS membranes but the quality of the control experiment is not as good as expected on the basis of the results obtained on Si. The intensity of the amide II band smoothly increases due to non-specific interactions. A possible explanation of the onset of these non-specific interactions only in the Ge case is related to factors as the quality of the chemical functionalization of the surface and the homogeneity of

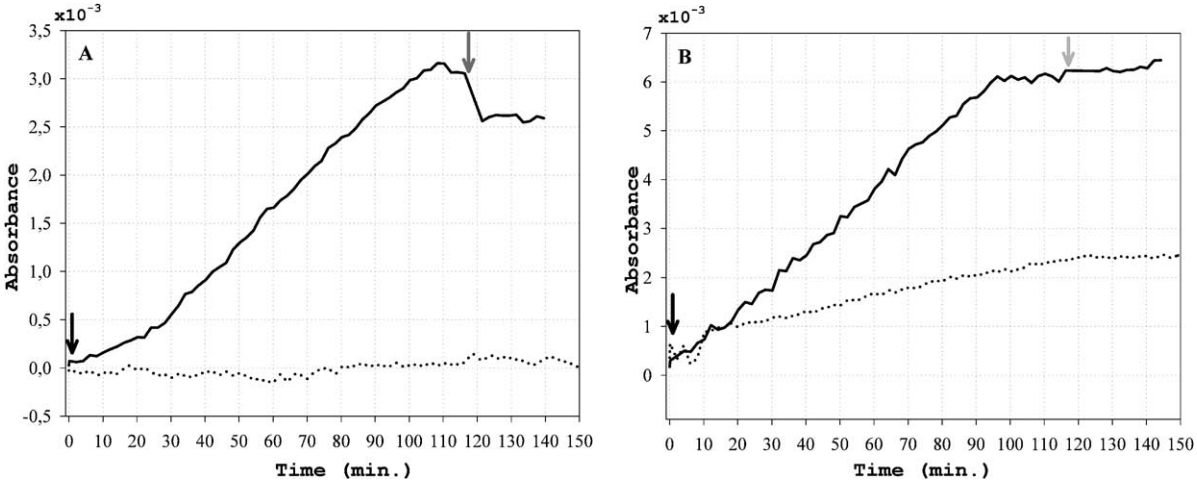

Fig. 10. Time evolution of the amide II band integrated intensity for the F_{VIII} binding to the lipid membranes on the OTS/Si (A) and on the OTS/Ge (B) crystals. The plain lines show the interaction with PS membranes whereas dotted lines fellow the interaction with the PC membranes. The arrows mark the beginning of the successive injection of the F_{VIII} and the buffer solutions (see Fig. 9).

the lipid layer. From our previous results (Fig. 1 and [19]), it is well known that the chemical grafting of OTS on Germanium is not straightforward due to the chemical reactivity of the Ge/GeO_2 surface which fundamentally differs from the reactivity of the Si/SiO_2 one and that hydrophobicity of the OTS-grafted Ge surfaces is slightly less than the hydrophobicity of the sylanized Silicon surfaces. Therefore, obtaining homogeneously OTS-grafted Ge surfaces remains a challenge. Nevertheless, on both types of optical substrates, the molecular construction may be considered as relatively stable throughout the whole experiment: the rinsing of the sensors by F_{VIII}-free buffer solution (indicated by the grey vertical arrow on Fig. 10) only slightly modifies the intensity of the amide II band. The maximum loss of intensity is about 15% for PS/OTS/Si sensor. We notice also that because of the large sensor size, the monitored signal does not saturate, even after 120 min.

4. Conclusion

The present work deals with interesting new possibilities of making functionalized surfaces: new devices suitable for the investigation of ligand–receptor interactions were presented. In particular, the research focused on optical waveguides constituted by an attenuated total internal reflection (ATR) element, transparent in the infrared and whose surfaces were activated in a view of covalently binding a receptor. Silicon as well as germanium ATR elements were considered. The original method was based on the grafting of bifunctional spacer molecules at the surface of the crystal, avoiding the deposition of an intermediate metal layer. The grafting of these binding molecules (under their N-hydroxysuccinimidyl ester forms) was performed by wet chemistry [18]. The functionalized surfaces were successfully used, e.g., for the detection of proteins (as factor VIII) binding to the phospholipid membranes. These experiments confirm the specificity of the F_{VIII}–PS interaction and the good establishment of the phosphatidyl membrane particularly over OTS-grafted Si plat.

Acknowledgements

This research has been supported by the Ministère de la Région Wallonne (WDU Program no. 14587, BIA-ATR project). The authors thank all the members of this Belgian consortium.

References

[1] E. Goormaghtigh, V. Raussens and J.M. Ruysschaert, Attenuated total reflection infrared spectroscopy of proteins and lipids in biological membranes, *Biochem. Biophys. Acta* **1422** (1999), 105–185.
[2] N.J. Harrik, *Internal Reflection Spectroscopy*, Wiley, New York, 1967.
[3] D.G. Buerk, *Biosensors: Theory and Applications*, Technomic Publishing Company, Inc., Lancaster, USA, 1993.
[4] P. Wenzl, M. Fringeli, J. Goette and U.P. Fringeli, Supported phospholipid bilayers prepared by the "LB/Vesicle Method": A Fourier transform infrared attenuated total reflection spectroscopic study on structure and stability, *Langmuir* **10** (1994), 4253–4264.
[5] J. Mou, D.M. Czajkowsky and Z. Shao, Gramicidin A aggregation in supported gel state phosphatidylcholine bilayers, *Biochemistry* **35** (1996), 3222–3226.
[6] J. Marchand-Brynaert, E. Goormaghtigh, F. Homble, M. Voue and J. De Coninck, Surface chemical modification of optical elements for the spectroscopic detection of molecules and organic components, PCT WO 02/056018A1, 2002.
[7] P.C. Spiegel, S.M. Kaiser, J.A. Simon and B.L. Stoddard, Disruption of protein–membrane binding and identification of small-molecule inhibitors of coagulation factor VIII, *Chem. Biol.* **11** (2004), 1413–1422.
[8] G.M. Bhopale and R.K. Nanda, Blood coagulation factor VIII: An overview, *J. Biosci*. **28** (2003), 783–789.
[9] H. Wakabayashi, Q. Zhou, K. Nogami, C. Ansong, F. Varfaj, S. Miles and P.J. Fay, pH-dependent association of factor VIII chains: Enhancement of affinity at physiological pH by Cu^{2+}, *Biochim. Biophys. Acta* **1764** (2006), 1094–1101.
[10] E. Saenko, A. Sarafanov, N. Greco, M. Shima, K. Loster, H. Schwinn and D. Josic, Use of surface plasmon resonance for studies of protein–protein and protein–phospholipid membrane interactions application to the binding of factor VIII to von Willebrand factor and to phosphatidylserine-containing membranes, *J. Chromatogr. A* **852** (1999), 59–71 (and Erratum in **872** (2000), 323).
[11] E.L. Saenko, D. Scandella, A.V. Yakhyaev and N.J. Greco, Activation of factor VIII by thrombin increases its affinity for binding to synthetic phospholipid membranes and activated platelets, *J. Biol. Chem.* **273** (1998), 27918–27926.
[12] E.M. Bevers, P. Comfurius and R.F. Zwaal, Changes in membrane phospholipid distribution during platelet activation, *Biochim. Biophys. Acta* **736** (1983), 57–66.
[13] R.D. Miclea, P.R. Varma, A. Peng and S.V. Balu-Iyer, Development and characterization of lipidic cochleate containing recombinant factor VIII, *Biochim. Biophys. Acta* **1768** (2007), 2890–2898.
[14] V.S. Purohita, K. Ramania, R.S. Kashib, M.J. Durranib, T.J. Kreigerb and S.V. Balasubramanian, Topology of factor VIII bound to phosphatidylserine-containing model membranes, *Biochim. Biophys. Acta* **1617** (2003), 31–38.
[15] W. Wang, Y.J. Wang and D.N. Kelner, Coagulation factor VIII: structure and stability, *Int. J. Pharm.* **259** (2003), 1–15.
[16] D. Scandella, G.E. Gilbert, M. Shima, H. Nakai, C. Eagleson, M. Felch, R. Prescott, K.J. Rajalakshmi, L.W. Hoyer and E. Saenko, Some factor VIII inhibitor antibodies recognize a common epitope corresponding to C2 domain amino acids 2248 through 2312, which overlap a phospholipid-binding site, *Blood* **86** (1995), 1811–1819.
[17] E. Saenko, A. Sarafanov, N. Ananyeva, E. Behre, M. Shima, H. Schwinn and D. Josic, Comparison of the properties of phospholipid surfaces formed on HPA and L1 biosensor chips for the binding of the coagulation factor VIII, *J. Chromatogr. A* **921** (2001), 49–56.
[18] K. Pflegerl, R. Hahn, E. Schallaun, D. Josic and A. Jungbauer, Quantification of plasma-derived blood coagulation factor VIII by real-time biosensor measurements, *J. Chromatogr. B* **752** (2001), 335–347.
[19] M. Voue, E. Goormaghtigh, F. Homble, J. Marchand-Brynaert, J. Conti, S. Devouge and J. De Coninck, Biochemical interaction analysis on ATR devices: A wet chemistry approach for surface functionalization, *Langmuir* **23** (2007), 949–955.
[20] S. Semal, M. Voue, J. Dehuit, M. de Ruijter and J. De Coninck, Dynamics of spontaneous spreading on heterogeneous surfaces in the partial wetting regime, *J. Phys. Chem. B* **103** (1999), 4854–4861.